

Article

An Analysis on the Characteristics and Influence Factors of Soil Salinity in the Wasteland of the Kashgar River Basin

Sheng Li, Li Lu *, Yuan Gao, Yun Zhang and Deyou Shen

School of Geology and Mining Engineering, Xinjiang University, Urumqi 830046, China; lisheng2997@163.com (S.L.); gaoyuan0511@live.cn (Y.G.); zyun0224@163.com (Y.Z.); sdy2643109541@163.com (D.S.)

* Correspondence: luli0401@sina.com; Tel.: +86-132-9555-5923

Abstract: Clarifying the salt ion composition characteristics and the influence factors of soil salinization of the wasteland in the Kashgar River Basin is of high importance for saline land improvement and utilization in this region. We studied the characteristics and influence factors of soil salinity in the wasteland of the Kashgar River Basin through classical statistics, principal component analysis and grey relational theory. The results showed that the total salt content had a T-shaped distribution pattern in the soil profile. As the most important ions, Cl^- , Na^+ , and SO_4^{2-} have the characteristics of vertical differentiation from top to bottom in the soil profile. Correlation analysis showed that the total salt content was negatively correlated to the HCO_3^- content and positively correlated to other salt ions, The most correlated anions were SO_4^{2-} and Cl^- . Na^+ , the most important cation, had the closest relationship with Cl^- , followed successively by SO_4^{2-} and HCO_3^- . Principal component analysis showed that SO_4^{2-} , total salt content, Na^+ , Cl^- , Mg^{2+} , and Ca^{2+} could represent soil salinity status and salt ion composition, while HCO_3^- could represent soil alkalization status. The grey relational analysis indicated a differentiation in the intensity of influence of each factor on soil salinization at different depths. Except for groundwater burial depth and elevation, the relational degree between other influence factors and soil salt content decreased with depth. Our research findings offer important clues for understanding the soil salinity characteristics and influence factors of salinization in the wasteland of the Kashgar River Basin.

Keywords: Kashgar River Basin; soil salinity characteristics; principal component analysis; grey relational analysis



Citation: Li, S.; Lu, L.; Gao, Y.; Zhang, Y.; Shen, D. An Analysis on the Characteristics and Influence Factors of Soil Salinity in the Wasteland of the Kashgar River Basin. *Sustainability* **2022**, *14*, 3500. <https://doi.org/10.3390/su14063500>

Academic Editor: Othmane Merah

Received: 19 January 2022

Accepted: 15 March 2022

Published: 16 March 2022

Publisher's Note: MDPI stays neutral with regard to jurisdictional claims in published maps and institutional affiliations.



Copyright: © 2022 by the authors. Licensee MDPI, Basel, Switzerland. This article is an open access article distributed under the terms and conditions of the Creative Commons Attribution (CC BY) license (<https://creativecommons.org/licenses/by/4.0/>).

1. Introduction

The Kashgar River Basin is one of the most important producing areas for grain, melons, and cotton in southern Xinjiang. Due to its special climate, topography, hydrogeology, and other conditions, the ecological environment of the river basin has become very fragile [1]; coupled with unreasonable human land development, imperfect irrigation and drainage facilities and years of poor maintenance of the cultivated land have resulted in a barren landscape with low soil self-regulation ability and severe salinization, causing large areas of different types of wasteland [2,3] which both restricts the sustainable development of local agriculture and adversely affects national food and ecological security [4–6].

To efficiently manage and utilize the large-scale salt wasteland, it is necessary to first understand the distribution of salt ions in the wasteland soil and the main types of salt as well as the relationship between them and the reasons for salinization [7,8]. Due to complexity, regionality, and differences in the formation and development of saline soil composition, it is difficult to study soil salinization [9,10]. However, the wide application of remote sensing and PCA in soil and hydrology in recent years has provided new ideas for the study of soil salinization [11]. PCA is a statistical analysis method that converts multiple indicators into a few comprehensive indicators, and is mostly used for the evaluation of

soil metal pollution and water quality. For example, A. Rezaei [12,13] used the principal component analysis method to comprehensively evaluate soil heavy metal pollution in mining areas in southeastern Iran based on sample data, and Mario Maiolo [14] conducted a multivariate analysis of water quality data on the drinking water supply system according to chemical–physical parameters collected in the Emilia Romagna region from 2013 to 2022. In the study of the properties of soil salinity, PCA generally reflects the properties of soil salinity by constructing one or a few comprehensive indicators, and rarely uses a linear combination of principal components and salinity variables to comprehensively evaluate the degree of soil salinization [15,16]. Li [17] used remote sensing imagery to combine retrieved salinity data with field sample data in order to analyze the effects of soil water content, surface temperature, and groundwater salinity on soil salinity in the oasis of Weigan River and Kuqa River. Ding [18] and Wu et al. [19] used years of remote sensing imagery to study dynamic changes in the influencing factors of soil salinization by constructing a soil salinization remote sensing monitoring model. In these studies, scholars mostly use the grid weight superposition and correlation coefficient method to analyze the correlation between soil salinity and various factors. Compared with the above theoretical methods, the grey system can quantify this relationship in cases with less data and more uncertainty [20,21].

We conducted a field survey and sampling in the wasteland of the Kashgar River Basin. Classical statistics was combined with principal component analysis to investigate the accumulation characteristics and existing form of soil salts in the study area. The linear combinations of principal components and salt ion contents were further established in order to evaluate the salinization status of the wasteland in the river basin. Next, ArcGIS was combined with grey system theory to extract spatial distribution data on the influence factors of salinization, and the intensity of the influence of each factor was determined. Our findings shed light on soil salinization prevention and control in the study area.

2. Materials and Methods

2.1. An Overview of the Study Area

The study area is located in the southwestern part of the Xinjiang Uygur Autonomous Region along the western margin of the Tarim Basin, belonging to the Kashgar River Basin ($75^{\circ}30'0''\sim 78^{\circ}0'0''$ E, $38^{\circ}40'00''\sim 39^{\circ}50'00''$ N) [22]. The major landforms found in the study area are mountains, dejection cones, alluvial fans, and alluvial–diluvial plain. The study area has four distinct seasons and a long sunshine duration. The majority is located in alluvial–diluvial fan oases, with significant annual and daily temperature changes; the average precipitation over the years is 60.80–172.80 mm with strong evaporation, and the study area belongs to the warm temperate continental arid/semi-arid climate [22]. The main crops grown in the study area are cotton, maize, walnut, and jujube. The natural vegetation includes *Tamarix chinensis*, *Phragmites australis* L., *Kalidium foliatum*, and *Haloxylon ammodendron*.

2.2. Geological Setting

The Kashgar River basin is located in the composite unit of the east wing of the front arc of Eurasian “mountain” structure and the head of Pamir “evil” structure of Kunlun Mountain in the south, including the geosynclinal fold belt of the southern Tianshan Mountain vein, the Qiaerlong–Kurlang geosynclinal fold belt of the West Kunlun fold system, the Kelpin faulted upfold, and the Tarim depression of the Tarim Platform, with the boundary mostly bounded by regional folds or fault structures.

The quaternary system (Q) is widely distributed in Kashgar River, with the most intense human activities in the basin, and the thickness of the quaternary system changes from 100 to 800 m generally. The particles of quaternary loose sediments gradually become finer from north to south, from west to east, and from south to north, that is, the particles of pebbles > gravel > gravel sand > medium coarse sand > fine sand > silt (sandy loam) >

loam (loam) > clay tend to become finer in the plane direction. Vertically, the quaternary loose sediment particles are generally coarse at the top and fine at the bottom.

2.3. Sampling and Testing

Field sampling was conducted in the study area in April 2019, a month when large-scale irrigation activities in the Kashgar River Basin had not yet begun, the evaporation was strong, and the salinization was mostly typical and a representative performance in this study at this time of the year. Fifty-nine sampling sites were set up in this area (Figure 1); to be specific, the sampling point was chosen as the center and another four sampling sites were arranged at a radius of 10 m around the center to form a plum blossom-shaped pattern in order to help reduce variabilities in the soil. Soil samples were sampled in layers of 0–30 cm, 30–50 cm, and 50–80 cm by pedal original earth-drill (with a drill bit 1 cm long and 38 mm in diameter); the soil samples collected from five sampling points were mixed together and about 0.5 kg of the soil sample was preserved while the remaining soil was discarded by quartering. During the sampling process, changes in soil lithology as well as special landforms were recorded in detail. All soil sample bags were numbered and delivered to the laboratory where they were air-dried at room temperature. The soil samples were passed through a 2 mm sieve according to Soil Agricultural Chemical Analysis Methods [23] at a water-to-soil ratio of 5:1. After that, the contents of salt ions (Na^+ , Cl^- , HCO_3^- , SO_4^{2-} , Ca^{2+} , Mg^{2+} , CO_3^-) in the leachate were determined, Cl^- was determined by silver nitrate titration, Na^+ was determined by flame photometry, HCO_3^- and CO_3^- were determined by sulfuric acid titration, SO_4^{2-} was determined by barium sulfate turbidimetric method, Ca^{2+} and Mg^{2+} were determined by atomic absorption spectrophotometry, and the average soil salt concentration was determined by the method of dyeing residues. The groundwater burial depth and groundwater mineralization data were provided by Xinjiang Survey and Design Institute of Water Resources and Hydropower, with the specific data shown in Table 1.

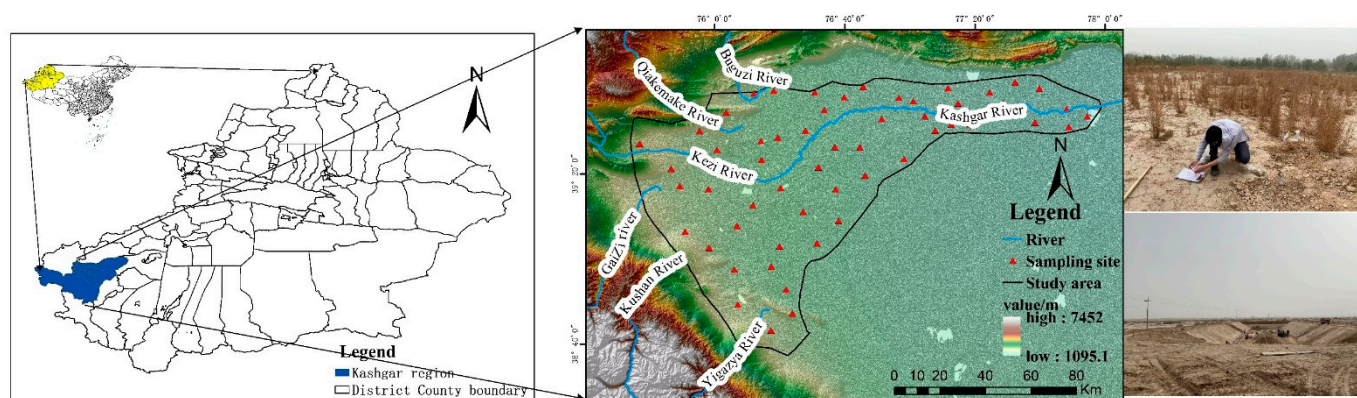


Figure 1. Geographical location of the study area and distribution of the sampling sites.

Table 1. Groundwater burial depth and groundwater mineralization data for the research area.

Number	X	Y	Groundwater Burial Depth (m)	Number	X	Y	TDS (g/L)
P1	576,503.9	4,339,705	1.76	T1	521,419	4,395,787	1.49
P2	576,067.3	4,341,260	3.20	T2	551,422	4,333,444	0.49
P3	572,194.8	4,340,068	8.05	T3	569,524	4,347,986	0.52
P4	570,566	4,340,270	11.46	T4	572,809	4,373,554	1.02
P5	571,251.3	4,341,927	4.11	T5	604,183	4,395,259	1.26
P6	568,459.7	4,340,613	20.12	T6	595,398	4,403,998	1.17
P7	571,176.9	4,335,633	5.34	T7	600,952	4,337,318	1.39
P8	570,073.5	4,330,381	30.75	T8	607,306	4,346,779	1.33

Table 1. Cont.

Number	X	Y	Groundwater Burial Depth (m)	Number	X	Y	TDS (g/L)
P9	570,264.3	4,328,847	48.92	T9	624,084	4,310,997	6.45
P10	567,675.8	4,331,748	28.50	T10	721,204	4,400,790	5.89
P11	565,266.4	4,331,850	54.17	T11	648,874	4,393,063	4.50
P12	563,712.4	4,332,452	65.83	T12	750,909	4,395,248	3.20
P13	574,753.9	4,333,682	7.05	T13	687,943	4,327,718	1.90
P14	551,439.3	4,326,612	13.03	T14	688,603	4,335,264	2.21
P15	553,684.7	4,331,917	1.61	T15	646,943.1	4,388,385	0.92
P16	557,701.6	4,336,541	105.10	T16	588,504.8	4,340,160	1.11
P17	546,555.3	4,341,241	10.63	T17	582,526.9	4,371,066	1.17
P18	540,204.2	4,351,757	4.00	T18	567,963.6	4,354,125	1.47
P19	541,025.1	4,350,185	10.45	T19	603,647.1	4,303,917	0.74
P20	540,813.9	4,350,597	5.00	T20	651,399	4,345,700	0.69
P21	540,548.1	4,351,105	1.40	T21	588,620.3	4,364,715	1.46
P22	539,247.5	4,350,885	7.70	T22	581,873	4,377,439	1.40
P23	538,938	4,351,492	7.78	T23	598,054	4,369,175	0.75
P24	538,620.9	4,352,119	5.60	T24	615,971	4,376,856	3.22
P25	551,590.6	4,346,056	22.18	T25	583,711	4,353,122	0.54
P26	549,239.8	4,348,063	23.44	T26	621,565	4,330,577	1.95
P27	548,058.2	4,349,225	25.38	T27	595,863	4,356,778	2.92
P28	546,971.1	4,345,715	3.98	T28	605,785	4,333,340	0.79
P29	549,476	4,353,536	23.44	T29	622,495	4,354,005	2.01
P30	550,352.9	4,352,758	20.00	T30	603,338	4,301,754	0.62
P31	553,354.6	4,352,854	10.85	T31	615,075	4,295,870	2.42
P32	559,470.7	4,350,702	9.50	T32	646,531	4,370,710	4.00
P33	568,492.7	4,344,105	7.60	T33	654,327	4,386,351	2.00
P34	564,526	4,347,754	4.16	T34	650,974	4,362,372	0.47
P35	565,335.2	4,349,674	4.02	T35	622,121	4,361,064	1.82
P36	567,734.6	4,352,880	7.55	T36	649,520	4,378,172	6.55
P37	565,471.6	4,355,390	16.00	T37	665,699	4,371,435	3.67
P38	570,648.8	4,347,131	2.50	T38	636,542	4,379,722	0.98
P39	572,924.5	4,349,146	2.70	T39	645,213	4,342,517	1.32
P40	574,453.5	4,351,030	2.70	T40	625,995	4,349,495	5.56

2.4. Processing Method

2.4.1. Remote Sensing Images

The Landsat 8 satellite images and digital elevation model (DEM) data used for the study were downloaded from a cloud-based data management platform in 10 September 2020 (<http://www.gscloud.cn>) and had a resolution of 30 m.

2.4.2. Statistical Analysis

Correlation analysis and principal component analysis were performed for soil salinity and constituent ions at the sampling sites using IBM SPSS Statistics 23.0 and Excel 2019.

Principal Component Analysis

Principal component analysis is a multivariate statistical method that reconstitutes the original indexes into a new group of unrelated comprehensive indexes to replace the original indexes by solving the principal components, and uses several comprehensive indexes to reflect the original indexes. Suppose there are n samples and each sample has p indicators, which are recorded as X_1, X_2, \dots, X_p . The main calculation steps of principal component analysis are as follows:

- (1) Establish the original database.
- (2) Standardize the original data and use the Z-score method to make standard changes to the data:

$$C_{ij} = \frac{x_{ij} - x_j}{S_j} \quad (1)$$

$$X = \begin{bmatrix} x_{11} & \cdots & x_{1p} \\ \vdots & \ddots & \vdots \\ x_{1n} & \cdots & x_{np} \end{bmatrix} \quad (2)$$

$$s_j^2 = \frac{\sum_{i=0}^n x(x_{ij} - x_j)^2}{n-1} \quad (j = 1, 2, \dots, p) \quad (3)$$

where x_{ij} is the value of the j -th index of the i -th partition and x_j, S_j are the sample mean and sample standard deviation of the j -th index, respectively.

- (3) Find the correlation coefficient matrix,

$$R = (r_{jk})_{pp} \quad (j, k = 1, 2, \dots, p) \quad (4)$$

where r_{jk} is the correlation coefficient of indexes j and k .

- (4) Find the eigenvalue and eigenvector of correlation matrix R and determine the principal component. If the characteristic value is recorded as $\lambda_1 \geq \lambda_2 \geq \dots \geq \lambda_m \geq 0$, the corresponding unit eigenvector is

$$a_i = (a_{1i} \ a_{2i} \ \dots \ a_{pi}) \quad (5)$$

Convert the standardized index variables into main components:

$$Z_i = a_{1i} C_1 + a_{2i} C_1 + \dots + a_{pi} C_p \quad (i = 1, 2, \dots, p) \quad (6)$$

where Z_1 is the first principal component, Z_2 is the second principal component, \dots ; thus, Z_p is the p -th principal component.

- (5) Calculate the variance contribution rate and determine the number of principal components. Generally, the number of principal components is equal to the number of original indicators; if the number of original indicators is large, it will be troublesome to conduct comprehensive evaluation. The method of principal component analysis is to select as few k principal components ($k < p$) as possible for comprehensive evaluation while at the same time making the amount of information lost as little as possible.

The contribution rate of the K value from cumulative variance $E = \frac{\sum_{i=1}^k \lambda_i}{\sum_{i=1}^p \lambda_i} \geq 75\%$, that is, select the minimum k with $E \geq 75\%$.

- (6) Comprehensive evaluation of K principal components. First find the linear weighted value of each principal component, $Z_i = a_{1i} C_1 + a_{2i} C_1 + \dots + a_{pi} C_p$, ($i = 1, 2, \dots, k$), Then, the weighted sum of k principal components is obtained to find the final evaluation value: $Z = e_i Z_i$, ($i = 1, 2, \dots, k$) where weight, e_i , is the contribution rate of each principal component variance; thus, $e_i = \lambda_i / \sum_{i=1}^p \lambda_i$.

Correlation Analysis

The measure of the degree of linear correlation between two variables is called the simple correlation coefficient (or single correlation coefficient). For two elements x and y , if their sample values are respectively, x_i, y_i ($i = 1, 2, \dots, n$), then the correlation coefficient (r_{xy}) between them is defined as

$$r_{xy} = \frac{\sum_{i=1}^n (x_i - \bar{x})(y_i - \bar{y})}{\sqrt{\sum_{i=1}^n (x_i - \bar{x})^2} \times \sqrt{\sum_{i=1}^n (y_i - \bar{y})^2}} \quad (7)$$

2.4.3. Spatial Data Vectorization

The geographical statistics function was run in ArcGIS to analyze the spatial differentiation structure of groundwater mineralization and burial depth in the study area, and the optimal theoretical model fitted using the variation function was employed for Kriging interpolation to generate the spatial distribution data of groundwater burial depth and mineralization in the study area. ArcGIS 3D Analyst was applied to the DEM data to extract the grid data of the slope in the study area. Landsat-8 optical remote sensing data, which were of the same time period as the field sampling and had undergone atmospheric correction, radiation correction, and geometric correction, were used for land surface temperature inversion. ERDAS software was utilized for the supervised classification of remote sensing images of the same period; in addition, by reference to China's national standards for land use classification and the actual situation of the study area, we divided the land into the following land use categories: bare land, saline land, shrubbery, low-coverage grassland, and medium-coverage grassland.

2.4.4. Grey Relational Analysis

Grey relational analysis is a multi-factorial statistical analysis method which calculates the similarity between the reference sequence and the comparison sequence; the more similar the two curves, the closer the relation between the sequence will be. This method can be used to quantify the intensity of relation and mutual influence of different factors in a system. The specific methods are as follows [24,25]:

- (1) Original data transformation. The selected indicators are different in physical meanings and dimensions, and we should thus adopt the method of removing dimension before comparing each data column. Each sub-sequence has different effects on the parent sequence; in this paper, we adopted the method of maximum standardization when quantifying standardization of various indicators. For example, there are indicators of positive correlation, such as $y_i = x_i/x_0$, and indicators of negative correlation, such as $y_i = (x_0 - x_i)/x_0$, where x_i is the actual value of the sub-sequence and x_0 is its maximal value.
- (2) Correlation coefficient computations. It is necessary to determine the correlation coefficient $\xi_i(k)$ in each sub-sequence $X_i(k)$ and parent sequence $X_0(k)$. The computational formula of correlation coefficient in the Grey System is as follows:

$$\xi_i(k) = \frac{\min_i \min_k |x_0(k) - x_i(k)| + \rho \max_i \max_k |x_0(k) - x_i(k)|}{|x_0(k) - x_i(k)| + \rho \max_i \max_k |x_0(k) - x_i(k)|} \quad (8)$$

among which: $k = 0, 1, 2, 3, \dots, N$, $i = 0, 1, 2, \dots, 7$, and $\xi_i(k)$ is the correlation coefficient of the data series of x_i and x_0 at position k . The effect of $\rho \in [0, 1]$, which is called the resolution ratio, is to highlight the difference between the correlation coefficients. Generally, the resolution ratio is 0.5 [20].

- (3) Solving the correlation degree, r_i . The correlation degree of the two sequences is provided by the average value of the correlation coefficient between the sub-sequence and the parent sequence at each time, that is,

$$r_i = \overline{\xi_i(k)} = \frac{1}{n} \sum_{k=1}^N \xi_i(k) \quad (9)$$

where r_i is the correlation degree between the two sequences and N is the number of each sub-sequence.

3. Results and Discussion of Research

3.1. Analysis of Soil Salt and Ion Content

It can be seen from Table 2 that the average pH of the soil is higher than 8, indicating that the soil is weakly alkaline. The average value of total salt content increases gradually from the deeper layers to topsoil and shows a T-shaped distribution, with the average total salt content of 0 to 30 and 30 to 50 cm soils greater than 20 g/kg and that of 50 to 80 cm soils between 10 and 20 g/kg. According to the local soil salinization classification standard in Xinjiang [26] shown in Table 3, the 0 to 30 and 30 to 50 cm soil horizon are saltierra, and the 50 to 80 cm horizon is severely salinized. Soil salinity is often classified according to the $\text{Cl}^-/\text{SO}_4^{2-}$ concentration ratio [27]; in the study area, the $\text{Cl}^-/\text{SO}_4^{2-}$ concentration ratios of all three horizons were between 0.2–1, and therefore the soil salinity of the wasteland was roughly classified as a chloride–sulfate, which means that the soil salts were predominantly sulfates and chlorides. The radial plot of soil ions (Figure 2) [28] shows that Cl^- , Na^+ , and SO_4^{2-} have vertical differentiation characteristics from top to bottom in the soil profile; in contrast, the contents of other salt ions changed much less significantly in the soil profile. These results indicate that if the climate is dry with little rain and strong evaporation, the salt ions in the wasteland of the river basin tend to accumulate in the surface soil and the soil is rarely washed. In terms of the anions, SO_4^{2-} has the highest content in all three soil horizons followed by Cl^- and HCO_3^- ; however, the vertical differentiation ability of SO_4^{2-} is not as good as that of Cl^- . The content of Na^+ in each layer of cation is the largest, followed by the content of Ca^{2+} , and the content of Mg^{2+} is the lowest (Figure 3).

Table 2. Statistical analysis of salt elements in soil profile.

Quantity	Soil Depth/cm	$\text{Cl}^-/\text{SO}_4^{2-}$	pH	Total Salt (g/kg)
59	0–30	0.859	8.6	43.64
55	30–50	0.569	8.5	32.29
57	50–80	0.514	8.2	15.82

Table 3. Classification standard of soil salinization degree in Xinjiang [26].

Classification	Non-Salinization	Mild Salinization	Moderate Salinization	Severe Salinization	Saltierra
Total salt (g/kg)	<3	3~6	6~10	10~20	>20

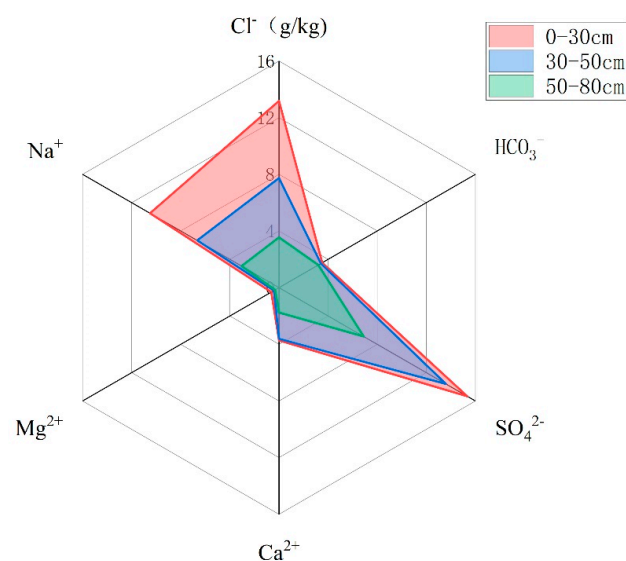


Figure 2. Radial diagram of salt ions in the study area [28].

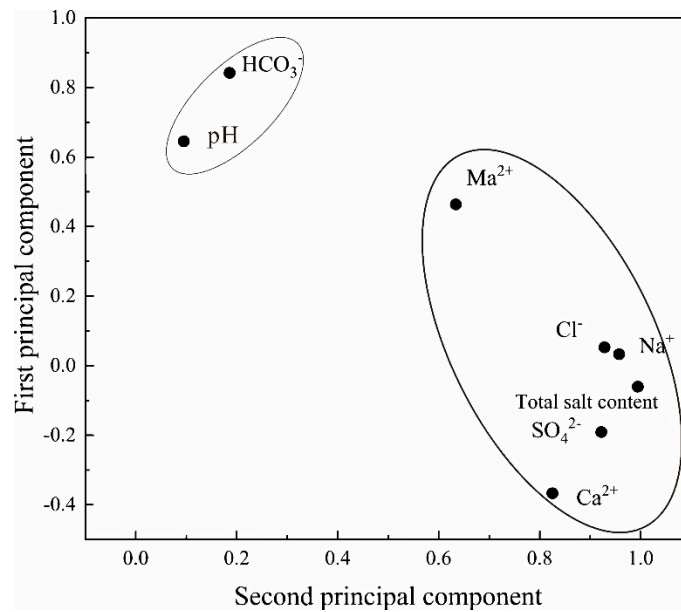


Figure 3. Two dimensional factors: load diagram of variable soil salinity.

3.2. Descriptive Statistics and Correlation Analysis of Salt Ions

Because CO_3^{2-} content is too low, and too low an ion content will cause distortion of coefficient of variation, HCO_3^- was used in place of soil $\text{CO}_3^{2-} + \text{HCO}_3^-$. The variabilities of salt ion contents across the horizons were compared in order to better understand the differences in the distribution characteristics and migration speeds of different ions in the soil profile [10]; therefore, this paper took the whole section as the research object.

Significant spatial variability in salt ion contents can be observed from Table 4, which might be attributed to the groundwater environment and land use type of the study area. Among the cations, the coefficient of variation was the highest for Na^+ , among the anions, the coefficient of variation was the highest for Cl^- , and the contents of both two salt ions showed strong variability. The coefficient of variation was lower for SO_4^{2-} , Ca^{2+} , and Mg^{2+} , and was the lowest for HCO_3^- ; this is similar to the results of previous studies [29]. The reason may be that the vegetation coverage of the wasteland is low and the surface temperature is high; thus, under strong evaporation the soluble salts in soil and groundwater rise with capillary water, and due to the different adsorption capacity of different ions and soil colloids they have different variability and differentiation capacity in the soil profile. Among them, Cl^- is a conservative ion and Na^+ is not easily adsorbed by soil clay; therefore, the coefficient of variation is the largest on the soil profile and is easy to accumulate on the surface. HCO_3^- , SO_4^{2-} , Ca^{2+} , and Mg^{2+} are affected by ion charge, hydration radius, ion concentration, and other characteristics, have relatively strong adsorption abilities with soil colloids and relatively small spatial variation [30], and are distributed on the soil profile in a relatively even manner.

Table 4. Descriptive analysis of soil salts and constituent ions.

Item	Minimum (g/kg)	Maximum (g/kg)	Mean (g/kg)	Coefficient of Variation
Cl^-	0.134	94.43	8.066	1.995
HCO_3^-	0.118	0.476	0.214	0.348
SO_4^{2-}	0.247	80.16	11.891	1.121
Ca^{2+}	0.084	24.515	3.021	0.834
Mg^{2+}	0.022	3.477	0.455	1.08
Na^+	0.041	68.586	6.676	1.815
Total salt (g/kg)	0.078	226.36	30.35	1.446

A correlation analysis between soil salt ions can help to reveal the existing form and the coordinated migration of salt ions in soil [31]. The correlation coefficients between salt ions are presented in Table 5. It can be seen from Table 5 that the total salt content of the soil is positively correlated with the contents of Cl^- , SO_4^{2-} , Ca^{2+} , Mg^{2+} , and Na^+ with a significance level of 0.01. The pair of anions most strongly correlated is SO_4^{2-} and Cl^- , further indicating that sulfates and chlorides are important salts that cause soil salinization; both are negatively correlated with the content of HCO_3^- , with a significance level of 0.01. The hydrolysis of HCO_3^- is very likely to happen in soil solution, which further aggravates soil alkalinity; from another perspective, we can say that higher salt concentration to some extent helps to inhibit soil alkalinity [32]. Comparing the correlation degrees between salt ions, it was found that Ca^{2+} is positively correlated with Cl^- and SO_4^{2-} with a significance level of 0.01, and the coefficients of correlation were 0.620 and 0.948, respectively. As the cation with the highest content, Na^+ has the strongest correlation with Cl^- (0.989), followed by its correlation with SO_4^{2-} (0.796), which indicates that the coordinated migration of Na^+ and Cl^- is the strongest, followed by that of Na^+ and SO_4^{2-} . This is consistent with the results of previous studies [10]; in the process of salt moving up and down, chloride and sulfate are the most active substances, mostly in the forms of NaCl and Na_2SO_4 . Carbonate is a minor constituent and is relatively stable in the soil profile. This indirectly indicates that in the process of irrigating and salt-leaching, the leaching rate of chloride is faster than that of other salts; therefore, appropriate irrigation and washing help to reduce the Na^+ and Cl^- contents in the soil and thereby reduce soil salinity [33]. Except for the significant correlation with HCO_3^- , Na^+ , and Ca^{2+} , where the correlation with HCO_3^- was the strongest, the correlation between soil pH and other ions was not significant.

Table 5. Correlation Analysis between soil salinity and composition ions.

Item	Cl^-	HCO_3^-	SO_4^{2-}	Ca^{2+}	Mg^{2+}	Na^+	Total Salt (g/kg)
Cl^-	1						
HCO_3^-	0.143	1					
SO_4^{2-}	0.727 **	0.111	1				
Ca^{2+}	0.620 **	0.013	0.948 **	1			
Mg^{2+}	0.571 **	0.266 *	0.453 **	0.242	1		
Na^+	0.989 **	0.160	0.796 **	0.673 **	0.568 **	1	
pH	0.369	0.413 *	0.436	−0.402 *	−0.299	0.400 *	1
Total salt (g/kg)	0.945 **	−0.362 **	0.911 **	0.822 **	0.552 **	0.972 **	−0.427

Note: ** $p < 0.01$, indicating a significant difference; * $p < 0.05$, indicating a significant difference.

3.3. Principal Component Analysis of Salt Ions in the Soil

Due to variabilities of salt ion contents being significant, it was difficult to quantitatively describe the distributions of the various salts and their constituent ions [34]. We performed principal component analysis to identify representative salt factors in the soil and create new variables without causing a loss of the original information, and the principal components thus developed were then used to evaluate the salinized status of the wasteland in the study area to offer a reference for predicting salinity trends during further wasteland reclamation.

After linear transformation, the eigenvalues of the first two principal components were 4.711 and 1.132, both being above 1. The corresponding variance contribution rate was 67.298% and 18.802%, respectively, and the cumulative variance contribution rate was above 85%. These two principal components could cover most of the original data information [31], with the information loss being only 13.9%.

The factor loading matrix in Table 6 shows the degree of correlation between one salt variable and a specific principal component; the higher the loading, the stronger the correlation and the greater the ability of the principal component to cover the information carried by variable [35]. According to the factor loading matrix, SO_4^{2-} , total salt content,

Na^+ , Cl^- , Mg^{2+} , and Ca^{2+} were more strongly correlated with the first principal component, and the factor loadings were 0.922, 0.995, 0.957, 0.928, 0.614, and 0.825, respectively; these salt ions had a very significant positive correlation with the total salt content. From the above, we determined that these six salt variables could represent the salinized status of the soil and the salt ion composition. Therefore, the first principal component could replace the effect of eight variables, excepting only HCO_3^- and pH. The contribution rate of the first principal component was the largest, at 67.298%, which shows that the soil is mainly salinized. HCO_3^- and pH showed high correlation in the second principal component, and the factor load was 0.842 and 0.638; at the same time, HCO_3^- and pH showed high correlation, indicating that the second principal component had represented the characteristics of salinization of soil and replaced the role of HCO_3^- and pH in the soil.

Table 6. Factor loading matrix and factor score coefficient matrix of the principal component analysis.

Salt Variable	Factor Loading Matrix		Factor Score Coefficient Matrix	
	Principal Component 1	Principal Component 2	Principal Component 1	Principal Component 2
Total salt content	0.995	−0.061	0.211	−0.054
Cl^-	0.928	0.052	0.197	0.046
HCO_3^-	0.186	0.842	0.039	0.744
SO_4^{2-}	0.922	−0.191	0.196	−0.169
Ca^{2+}	0.825	−0.367	0.175	−0.325
Mg^{2+}	0.614	0.493	0.130	0.436
Na^+	0.957	0.033	0.203	0.029
pH	0.082	0.628	0.073	0.603

The factor loading plot of the first and the second principal components (Figure 3) further reflected that the salinity trend in wasteland of the Kashgar River Basin. Soil salinization was the primary process, while alkalization was secondary.

The coefficients of the principal component score were calculated based on all variables by linear regression analysis; in this way, we could use the linear combinations of principal components and original variables for salinization status evaluation of the wasteland, as shown in Table 6. Hence, we constructed the linear score equations between each principal component and the variables, as shown in Equations (10) and (11).

$$P_1 = 0.211X_1 + 0.197X_2 + 0.039X_3 + 0.196X_4 + 0.175X_5 + 0.130X_6 + 0.203X_7 + 0.073X_8 \quad (10)$$

$$P_2 = -0.054X_1 + 0.046X_2 + 0.744X_3 - 0.169X_4 - 0.325X_5 + 0.436X_6 + 0.029X_7 + 0.073X_8 \quad (11)$$

where P_1 and P_2 are the first and the second principal components, respectively, and X_1 , X_2 to X_7 , X_8 are eight salt variables, namely, total salt content and $\text{Cl}^- \dots \dots \text{Na}^+$. By integrating P_1 and P_2 , we further constructed the comprehensive evaluation function of the salinity status of the wasteland of the Kashgar River Basin. As shown in Equation (5), the coefficients in this comprehensive evaluation function were determined by dividing the contribution rate of each of the two principal components by the corresponding cumulative contribution rate.

$$F_1 = 0.781P_1 + 0.219P_2 = 0.153X_1 + 0.164X_2 + 0.194X_3 + 0.116X_4 + 0.066X_5 + 0.197X_6 + 0.165X_7 + 0.189X_8 \quad (12)$$

The coefficients in the equation above reflected the weights of the principal components and the salt variables in the comprehensive evaluation function; the greater the weights, the more important the variable in the model. The comprehensive score was calculated using Equation (12) for the sampling sites (in the entire soil profile) arranged in the wasteland of the study area; this score varied between 1.556 and 32.140 with an average of 6.20 and a coefficient of variation of 1.12, indicating a strong variation. This result offers

a theoretical reference for the comprehensive analysis and evaluation of soil salinity status in the wasteland of the Kashgar River Basin.

3.4. Analysis of the Influence Factors of Salinization

3.4.1. Choice of the Influence Factors of Soil Salinization

The influence factors of soil salinization include meteorological factors, comprehensive geo-science factors, and land management factors. The three types of factors are coupled and jointly act on the soil salinization process [36]. Among them, geo-science (altitude, slope) lays the comprehensive molecular foundation for the formation of salinization, meteorological (surface temperature) and land management factors (mode of land use) influence the trend of salinization, and the groundwater environment has a direct bearing on the salinization process via groundwater mineralization and groundwater burial depth. Therefore, we chose groundwater burial depth, groundwater mineralization, land use type, land surface temperature, elevation, and slope as sequences of influence, and extracted them in terms of their respective spatial variables (Figure 4a–f). The soluble salt content of the sampling point was used as the reference sequence, which was obtained from the indoor analysis results.

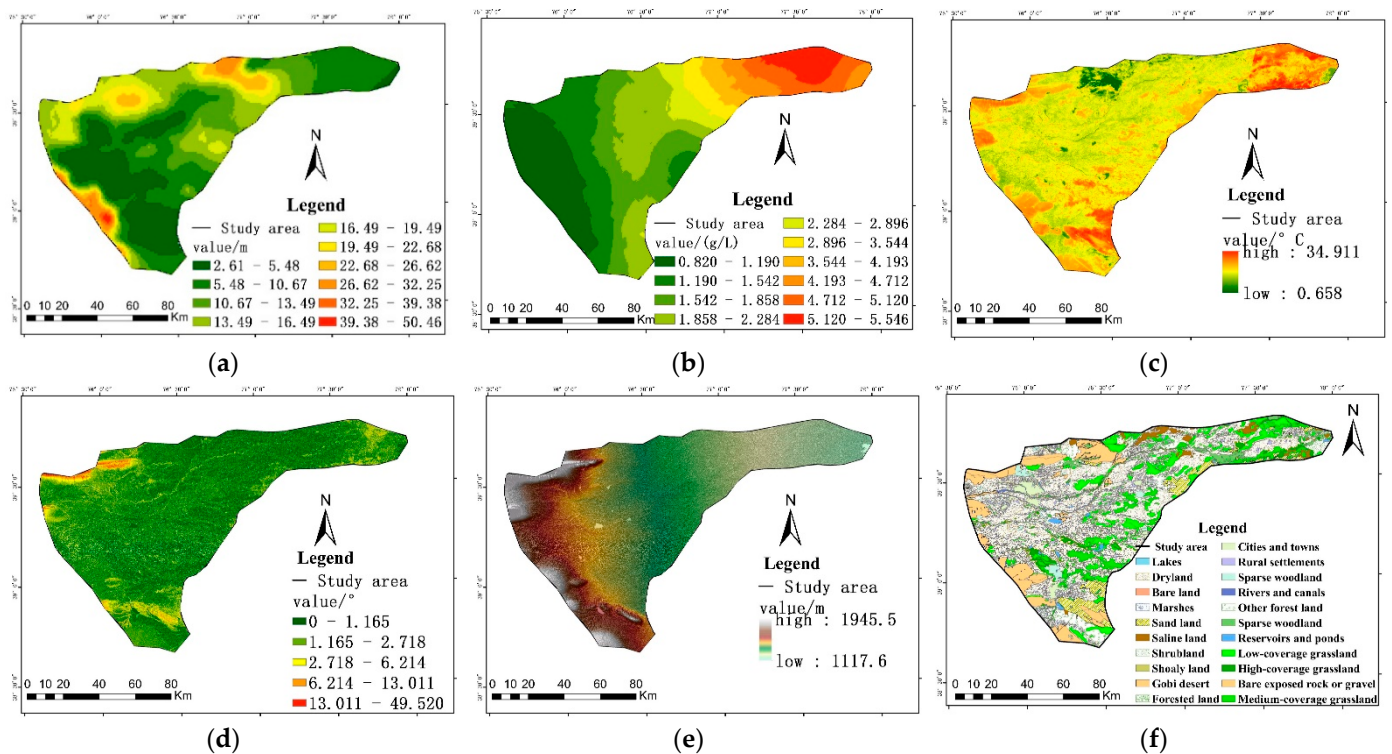


Figure 4. Spatial distribution data of the influence factors of salinization: Groundwater burial depth (a); Groundwater mineralization (TDS) (b); Land surface temperature (LST) (c); Topographic slope (d); Surface elevation (e); Land use type (LUP) (f).

3.4.2. Correlation Sequence and Analysis

We calculated the degree of correlation between six types of influencing factors and soil salt content at different depths according to Formulas (8) and (9), as shown in Table 7. In a grey system, the higher the grey relational coefficient, the greater the importance of the factor to salinization formation and evolution; as shown in Table 7, the six influence factors affected soil salinity at different depths in a significantly different manner. In the 0–30 cm horizon, the factors were ranked in descending order of the grey relational coefficient with the soil salt content as follows: land use type > groundwater mineralization > land surface temperature > elevation > groundwater burial depth > slope; in the 30–50 cm horizon, the

ranking was as follows: groundwater mineralization > land use type > elevation > land surface temperature > groundwater burial depth > slope; and in the 50–80 cm horizon, the ranking was as follows: groundwater mineralization > elevation > groundwater burial depth > land use type > land surface temperature > slope.

Table 7. Correlations between the influence factors of salinization at different depths.

Depth/cm	Subsequence					
	Groundwater Burial Depth	Groundwater Mineralization	Land Use Type	Land Surface Temperature	Slope	Elevation
0–30 cm	0.638	0.762	0.815	0.733	0.597	0.717
30–50 cm	0.609	0.723	0.683	0.617	0.503	0.631
50–80 cm	0.633	0.698	0.573	0.508	0.498	0.655

According to Table 7, at a greater soil depth the grey relational coefficient between all influence factors (except for groundwater burial depth and elevation) and the soil salt content gradually decreased; in other words, the 0–30 cm horizon was most susceptible to salinization, and the Grey System coefficients calculated for each influence factor in this horizon represented the sensitivity of each factor and indicated which factors played a greater role in the salinization of shallow soil. In the 0–30 cm horizon, the grey relational coefficients were above 0.7 for the land use type, groundwater mineralization, land surface temperature, and elevation; these four factors were dominant in the evolution of shallow soil salinization. The wasteland, where the soil samples were taken, is mostly composed of saline land, abandoned dryland, grassland, halophyte bush vegetation, and desert. The soil's physicochemical properties, land surface evaporation intensity (land surface temperature), and physiological characteristics of vegetation vary under different land use types, and it is inevitable that the spatial and temporal distributions of groundwater level and quality are uneven, which further results in differentiation in the intensity of influences on surface soil salinity [37–39]. Elevation has a direct impact on groundwater and surface water movement as well as on soil salt accumulation and elimination. As shown in Figure 4, the terrain is higher in the upper reach of the Kashgar River; where the groundwater mineralization is lower, the soil salt discharge is predominant, and the soil salt content is lower. As the groundwater and the surface water move downstream, groundwater mineralization increases and surface soil salinity is further aggravated under strong evaporation. The above findings agree with those by Li [40], Luo [41], and Zhang [42] regarding the influence factors of soil salinity in the Manas River Basin, the oasis of Weigan and Kuqa Rivers, and the Qitai Oasis, respectively.

Compared with surface soils, the relational degree of salt content in the deeper horizon (50–80 cm) with groundwater mineralization and burial depth was greater than that with land use type and land surface temperature. This is probably because the plants and their roots are shorter in the study area. As the roots cannot reach the deeper horizons, the land use type has a greater impact on the salt content of surface soils [17,43]. In areas with shallow buried groundwater, deeper soils are less affected by evaporation (land surface temperature), whereas the capillary action is stronger; thus, in this soil horizon, land use type and land surface temperature had a smaller impact on salinity than groundwater environment. This finding agrees with those of Fan et al. [38,44] In all three horizons, the soil salt content had a lower relational degree with slope, which was different from the results of Zhang et al. [35,42] The reason for this may be attributed to different terrain in different regions; our study area was located in an alluvial—diluvial plain oasis where the terrain and slope fluctuate less significantly. It can be seen from figure D that the slope is mostly 0–2.718°; therefore, the slope had a lower relational degree with salt content in each soil horizon.

4. Conclusions

Through the statistical analysis, it was found that the wasteland soil in the basin was severely salinized, and the type of saline soil was dominated by surface-aggregate chloride sulfate. There were significant differences in the content and variability of different ions, with Cl^- and SO_4^{2-} having the highest content and the greatest variability in anions, indicating that they are rarely affected by irrigation leaching, similar to the results from previous studies. Despite the low carbonate content, the alkalization of the soil is a possibility that should not be neglected. Correlation analysis found that the correlation between the total salt content and Cl^- , Na^+ , and SO_4^{2-} was the strongest. At the same time, the correlation between Na^+ and Cl^- and SO_4^{2-} were very significant, which reveals that NaCl and Na_2SO_4 were the main salts in the soil. Due to the easy leaching of chlorides and sodium salts, the contents of Cl^- , Na^+ , and SO_4^{2-} can be reduced by appropriate irrigation and leaching, and the salinization of such soils can be controlled. However, considering that HCO_3^- is negatively correlated with total salts, rinsing the salt to reduce soil salinity will increase HCO_3^- content and aggravate soil alkalinity. Therefore, it is necessary to select an appropriate irrigation water quality. The salinization process of the wasteland in the study area is the result of a combination of many factors. Therefore, to scientifically improve and utilize the saline soil in the basin, the focus should be on controlling the influencing factors of salinization in the basin. According to the grey relation analysis, the focus of soil salinity control is to strengthen land use management and prevent inappropriate land development from exacerbating salinization. At the same time, saline soils should be improved by planting salt-tolerant crops and utilizing their desalination effect while ensuring the quality of salt wash water, strengthening dynamic monitoring and regulation of groundwater, maintaining a reasonable groundwater level, and preventing the occurrence of secondary soil salinization caused by improper irrigation and drainage. Finally, the development of soil salinization during the treatment process can be comprehensively assessed through the comprehensive score model (12) constructed by the principal component to provide a scientific basis for subsequent salinization prevention and control.

This study revealed the correlation between total salts of soil and different salt ions, established a linear relationship between different salt ions and principal components, and clarified the influencing factors of salinization. These research results help to reveal the influence of different salt ions on soil salinity, which is the premise and basis for effective prevention and improvement of soil salinity and is of great theoretical and practical significance. In order to better understand the development trend and spatial distribution characteristics of soil salinization in the study area, it will be necessary to further study the spatiotemporal aspects of soil salinity in the next stage of research.

Author Contributions: Conceptualization, S.L. and L.L.; methodology, S.L., Y.G. and D.S.; software, L.L., Y.G. and Y.Z.; validation, Y.G., Y.Z. and L.L.; formal analysis, L.L. and D.S.; investigation, D.S.; resources, S.L.; data curation, Y.Z. and S.L.; writing—original draft preparation, L.L. and Y.G.; writing—review and editing, S.L. and D.S.; visualization, Y.G.; supervision, L.L. and S.L.; project administration, Y.Z.; funding acquisition, S.L. and Y.G. All authors have read and agreed to the published version of the manuscript.

Funding: This research received no external funding.

Institutional Review Board Statement: Not applicable.

Informed Consent Statement: Not applicable.

Data Availability Statement: Some data used during the study are available from the corresponding author by request (email: luli0401@sina.com (L.L.)).

Conflicts of Interest: The authors declare no conflict of interest.

References

1. Chen, Y.B.; Hu, S.J.; Luo, Y.; Tian, C.Y. Relationship between soil salt accumulation in abandoned surface layer and groundwater in shallow groundwater buried area of Kashgar, Xinjiang. *Acta Pedol. Sin.* **2014**, *51*, 75–81.
2. Pérez-Sirvent, C.; Martínez-Sánchez, M.J.; Vidal, J.; Sánchez, A. The role of low-quality irrigation water in the desertification of semi-arid zones in Murcia, SE Spain. *Geoderma* **2003**, *113*, 109–125. [[CrossRef](#)]
3. Niu, D.L.; Peng, H.C.; Wang, Q.J. The principal component analysis of salinized situation in desert land of Chaidamu basin. *Acta Pratac. Sin.* **2001**, *10*, 39–46.
4. Amezketa, E. An integrated methodology for assessing soil salinization, a pre-condition for land desertification. *J. Arid Environ.* **2006**, *67*, 594–606. [[CrossRef](#)]
5. Dehaan, R.; Taylor, G.R. Image-derived spectral endmembers as indicators of salinization. *Int. J. Remote Sens.* **2003**, *24*, 775–794. [[CrossRef](#)]
6. Singh, A. Soil salinization management for sustainable development: A review. *J. Environ. Manag.* **2020**, *277*, 111383. [[CrossRef](#)]
7. Zhao, W.; Zhou, Q.; Tian, Z.; Cui, Y.; Liang, Y.; Wang, H. Apply biochar to ameliorate soda saline-alkali land, improve soil function and increase corn nutrient availability in the Songnen Plain. *Sci. Total Environ.* **2020**, *722*, 137428. [[CrossRef](#)]
8. Wong, V.N.; Greene, R.S.B.; Dalal, R.C.; Murphy, B.W. Soil carbon dynamics in saline and sodic soils: A review. *Soil Use Manag.* **2010**, *26*, 2–11. [[CrossRef](#)]
9. Singh, K.; Mishra, A.K.; Singh, B.; Singh, R.P.; Patra, D.D. Tillage Effects on Crop Yield and Physicochemical Properties of Sodic Soils. *Land Degr. Dev.* **2016**, *27*, 223–230. [[CrossRef](#)]
10. Zhang, T.B.; Kang, Y.H.; Hu, W.; Dou, C.Y. A study on the salinity characteristics of cracked alkaline soil in Yinbei irrigation district of Ningxia based on principal component analysis. *Agric. Res. Arid Areas* **2012**, *30*, 39–46.
11. Aly, Z.; Bonn, F.J.; Magagi, R. Analysis of the Backscattering Coefficient of Salt-Affected Soils Using Modeling and RADARSAT-1 SAR Data. *IEEE Trans. Geosci. Remote Sens.* **2007**, *45*, 332–341. [[CrossRef](#)]
12. Rezaei, A.; Hassani, H.; Fard Mousavi, S.B.; Hassani, S.; Jabbari, N. Assessment of Heavy Metals Contamination in Surface Soils in Meiduk Copper Mine Area, SE Iran. *Earth Sci Malays.* **2019**, *3*, 2–8. [[CrossRef](#)]
13. Rezaei, A.; Hassani, H.; Fard Mousavi, S.B.; Jabbari, N. Evaluation of Heavy Metals Concentration in Jajarm Bauxite Deposit in Northeast of Iran Using Environmental Pollution Indices. *Malays. J. Geosci.* **2019**, *3*, 12–20. [[CrossRef](#)]
14. Maiolo, M.; Pantusa, D. Multivariate Analysis of Water Quality Data for Drinking Water Supply Systems. *Water* **2021**, *13*, 1766. [[CrossRef](#)]
15. Rezapour, S.; Kalashypour, E. Effects of irrigation and cultivation on the chemical indices of saline–sodic soils in a calcareous environment. *Int. J. Environ. Sci. Technol.* **2019**, *16*, 1501–1514. [[CrossRef](#)]
16. Acosta, J.A.; Faz, A.; Jansen, B.; Kalbitz, K.; Martínez-Martínez, S. Assessment of salinity status in intensively cultivated soils under semiarid climate, Murcia, SE Spain. *J. Arid Environ.* **2011**, *75*, 1056–1066. [[CrossRef](#)]
17. Li, Y.J.; Ding, J.L.; Gulmira, E. Soil salt distribution and the factors affecting it in the oasis of Weigan and Kuqa Rivers. *J. Irrig. Drain.* **2019**, *3*, 58–65.
18. Ding, J.L.; Yao, Y.; Wang, F. Spatial modeling of soil salinization in arid area. *Ecol. Environ.* **2014**, *34*, 12.
19. Wu, Z.; Yan, Q.; Zhang, S.; Lei, S.; Lu, Q.; Hua, X. Remote Sensing Monitoring of Soil Salinization Based on SI-Brightness Feature Space and Drivers Analysis: A Case Study of Surface Mining Areas in Semi-Arid Steppe. *IEEE Access* **2021**, *9*, 110137–110148. [[CrossRef](#)]
20. Liu, S.F. *Grey System Theory and Application*; Science Press: Beijing, China, 2010. (In Chinese)
21. Elias, J.N.; Shi, Q.D.; Abulah, A.; Xia, N. Quantitative evaluation of Soil Salinization Risk in Yutian Oasis by grey evaluation model. *Trans. Chin. Soc. Agric. Eng.* **2019**, *35*, 176–184.
22. Gulgine, H.; Muhtar, T.; Yu, K.; Elsidin, Y.; Aihematijiang, S. Analysis on the characteristics of saline soil of Kashghar river valley. *J. Arid Land Resour. Environ.* **2012**, *26*, 169–173.
23. Lu, R.K. *Soil Agricultural Chemical Analysis Method*; Chinese Agricultural Science and Technology Press: Beijing, China, 1999. (In Chinese)
24. Yao, R.J.; Yang, J.S.; Chen, X.B.; Yu, S.P. Study on risk assessment of soil salinization in typical reclamation area of coastal zone in Northern Jiangsu. *Chin. J. Eco-Agric.* **2010**, *18*, 1000–1006. [[CrossRef](#)]
25. Maitittuerxun, A.; Haimiti, Y.; Sun, H.I. Correlation analysis of the relationship between soil salinity and groundwater in Yili River Basin. *Chin. J. Soil Sci.* **2013**, *44*, 561–566.
26. Soil Survey Office of Uygur Autonomous Region of Xinjiang, Agricultural Bureau of Uygur Autonomous Region of Xinjiang. *Soil Xinjiang*; Science Press: Beijing, China, 1996. (In Chinese)
27. Li, T.J.; Zhao, Y.; Zhang, K.L. *Fundamentals of Soil Science and Soil Geography*; People’s Education Press: Beijing, China, 1983. (In Chinese)
28. Iqrahman, A.; Maimaiti, S.; Ma, C.Y. Spatial distribution characteristics of soil salinization in the oasis of Weigan and Kuqa Rivers. *China Rural Water Hydropower* **2020**, *8*, 110–116.
29. Jiao, Y.; Kang, Y.; Wan, S.; Sun, Z.; Liu, W.; Dong, F. Effect of soil matric potential on the distribution of soil salt under drip irrigation on saline and alkaline land in arid regions. *Trans. Chin. Soc. Agric. Eng.* **2008**, *24*, 53–58.
30. Xiong, S.G. *Basic Soil Science*; China Agricultural University Press: Beijing, China, 2001; pp. 185–187. (In Chinese)

31. Liang, D.; Li, X.G.; Asjem, T.; Lai, N. Salinity characteristics of soil profiles in the western lakeside of Bosten Lake, Xinjiang. *Agric. Res. Arid Areas* **2014**, *32*, 151–158.
32. Zhang, X.; Huang, B.; Liang, Z.W.; Zhao, Y.C.; Sun, W.X. A study on soil salinization characteristics in the western Songnen Plain. *Soils* **2013**, *45*, 1332–1338.
33. Ge, G. *Saline Alkali Land Improvement*; Water Resources and Electric Power Press: Beijing, China, 1987. (In Chinese)
34. Li, X.G. Analysis of spatial variation characteristics of topsoil salt in the oasis downstream of Kaidu River Basin: Case study of Yanqi County. *Geogr. Inform. Sci.* **2014**, *1*, 105–109.
35. Ainur, T. *Study on Spatial Variability of Soil Salts in the Bortala River Basin and Its Influence Factors*; Xinjiang University: Urumqi, China, 2013. (In Chinese)
36. Liu, Q.; He, Y.; Deng, W.; Zhang, G.X. A study on soil salinization process in a changing environment: A case study of the middle and lower reaches of the Taoer River. *J. Arid Land Resour. Environ.* **2005**, *06*, 115–119.
37. Du, B.C.X.; Cheng, Y.X.; Wu, L. Analysis of negative correlation between vegetation and soil salinization in Junggar Basin. *Acta Ecol. Sin.* **2021**, *23*, 1–13.
38. Jing, Y.P.; Li, Y.J.; Gao, W.; Li, X.P. Salinity characteristics of saline-alkali soil in Hetao Plain under different land use. *Res. Soil Water Conserv.* **2020**, *27*, 372–379.
39. Wang, X.M.; Chai, Z.P.; Tashpolat, T. Spatial heterogeneity of topsoil salinity in the delta oasis of Weigan and Kuqa rivers. *J. Arid Land Resour. Environ.* **2012**, *26*, 88–93.
40. Li, Y.Y.; Zhang, F.H.; Pan, X.D.; Chen, F.; Lai, X.Q. Changes of salt accumulation in soil layers with different landforms in Manas River Valley in Xinjiang Region. *Trans. Chin. Soc. Agric. Eng.* **2007**, *23*, 60–64.
41. Luo, J.Y. Study on the Impact Factors of Soil Salinization Based on 3S Technology. Master's Thesis, Xinjiang University, Urumqi, China, 2009; pp. 38–44. (In Chinese)
42. Zhang, F.; Xiong, H.G.; Tian, Y.; Nuan, F.M. Impacts of regional topographic factors on spatial distribution of soil salinization in Qitai Oasis. *Res. Environ. Sci.* **2011**, *24*, 731–739.
43. Liu, F.; Chen, P.Y.; Yu, H.C.; Ma, J.Z. Analysis of spatial distribution characteristics of soil water and salts under different land use types in Minqin Oasis. *Arid Zone Geogr.* **2020**, *43*, 406–414.
44. Fan, X.M.; Liu, G.H.; Tang, Z.P.; Shu, L.C. Analysis on main contributors influencing soil salinization of Yellow River Delta. *J. Soil Water Conserv.* **2010**, *24*, 139–144.